# Scheme to Probe Optomechanical Correlations between Two Optical Beams Down to the Quantum Level

P. Verlot, A. Tavernarakis, T. Briant, P.-F. Cohadon, and A. Heidmann

*Laboratoire Kastler Brossel, UPMC-ENS-CNRS, Case 74, 4 place Jussieu, F75252 Paris Cedex 05, France*

(Received 12 September 2008; published 10 March 2009)

The quantum effects of radiation pressure are expected to limit the sensitivity of second-generation gravitational-wave interferometers. Though ubiquitous, such effects are so weak that they have not been experimentally demonstrated yet. Using a high-finesse optical cavity and a classical intensity noise, we have demonstrated radiation-pressure induced correlations between two optical beams sent into the same moving mirror cavity. Our scheme can be used to retrieve weak correlations at the quantum level and has applications both in high-sensitivity measurements and in quantum optics.

DOI: 10.1103/PhysRevLett.102.103601 PACS numbers: 42.50.Wk, 03.65.Ta, 05.40.Jc

The quantum effects of optomechanical coupling, the radiation-pressure coupling between a moving mirror and an incident light field, were first studied in the framework of gravitational-wave detection [1,2], enforcing quantum limits to the sensitivity of large-scale interferometers [3]. Overcoming these limits [4] was a major motivation for the quantum optics experiments performed shortly thereafter, such as squeezing of the light field [5,6] or quantum nondemolition (QND) measurements [7]. Such pioneering experiments were performed with nonlinear optical media, but optomechanical coupling was soon proposed as a candidate nonlinear mechanism of its own [8–10], based upon correlations between light intensity and mirror displacement induced by radiation pressure.

The first experiments fell short of the quantum regime [11–13] and even though recent ones demonstrated a much larger optomechanical coupling [14–19], they mainly focused on the possible demonstration of the quantum ground state of a mechanical resonator [20]. To observe the optomechanical correlations, two beams have to be sent upon the moving mirror (see Fig. 1): the intensity fluctuations of the first, intense, signal beam drive the mirror into motion by radiation pressure, whereas the resulting position fluctuations are monitored through the phase of the second, weaker, meter beam. As the intensity fluctuations of the signal beam are unaltered by reflection upon the mirror and as far as the radiation pressure of the meter beam is negligible, the intensity-phase correlations observable between the two reflected beams provide a direct measurement of the optomechanical correlations.

To monitor these radiation-pressure effects down to the quantum level and hence perform a real-time QND measurement of the signal intensity via the meter phase [10], one has first to enhance the optomechanical coupling by using a high-finesse cavity with a moving mirror, as shown in Fig. 1. The position fluctuations $\delta x_{\mathrm{rad}}$ induced by the quantum intensity fluctuations of the signal beam also have to be the dominant noise source, which requires to lower the thermal fluctuations $\delta x_T$ of the moving mirror. For a harmonic oscillator of mass $M$, resonance frequency $\Omega_M/2\pi$, and mechanical quality factor $Q$, the corresponding ratio between the radiation pressure and thermal noise spectra can be written [10]

$$\frac{S_x^{\mathrm{rad}}}{S_x^T} \simeq 2.3\left(\frac{\mathcal{F}}{300\,000}\right)^2\left(\frac{800\ \mathrm{nm}}{\lambda}\right)\left(\frac{P_{\mathrm{in}}}{1\ \mathrm{mW}}\right)\left(\frac{1\ \mathrm{mg}}{M}\right)\left(\frac{Q}{10^6}\right) \times \left(\frac{1\ \mathrm{MHz}}{\Omega_M/2\pi}\right)\left(\frac{1\ \mathrm{K}}{T}\right), \quad (1)$$

where $T$ is the environment temperature, $\mathcal{F}$ the cavity finesse, $\lambda$ the optical wavelength, and $P_{\mathrm{in}}$ the incident intensity of the signal beam. The stated values have all already been achieved independently in various state-of-the-art optomechanical systems [14–19,21,22], but combining the favorable mechanical behavior of NEMS [21] with a very high optical finesse [22] is an even greater experimental challenge.

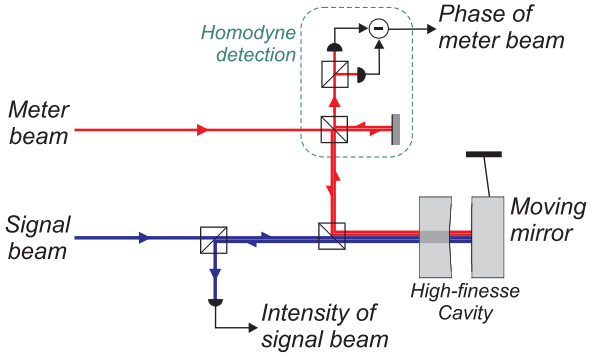


FIG. 1 (color online). Principle of the direct observation of optomechanical correlations. Both an intense signal beam and a weaker meter beam are sent into a resonant high-finesse cavity with a moving mirror. Intensity fluctuations of the signal beam are imprinted by radiation pressure onto the position fluctuations of the moving mirror, and, subsequently, onto the phase fluctuations of the meter beam. The two reflected beams then display intensity-phase correlations, retrieved with both a photodiode and a homodyne detection.

 

In this work, we report the observation of optomechanical correlations measured close to the quantum level. To reach a ratio (1) as large as possible, we favor the optical characteristics and use a fused silica moving mirror, which provides both a very high optical finesse [22] and mechanical quality factor [23], at the expense of a larger mass. The optomechanical correlations have then been measured with a tiny classical intensity modulation of the signal beam that mimics at a higher level its quantum fluctuations [22,24].

Our experimental setup is based on a single-ended optical cavity, with a 1-inch fused silica cylindrical input mirror. The moving mirror, used as end mirror, is a plano-convex 34-mm diameter and 2.5-mm thick mirror, which displays Gaussian internal vibration modes [23]. We work at frequencies close to a mechanical resonance with the following optomechanical characteristics, deduced from the thermal noise spectrum at room temperature: $\Omega_M/2\pi = 1.125$ MHz, $M = 500$ mg, $Q = 500\,000$.

The low roughness of the silica substrates allows for optical coatings with very low losses: we have obtained a cavity finesse $\mathcal{F} = 330\,000$, mainly limited by the 20-ppm transmission of the input mirror. This is crucial for quantum optics experiments for which loss has to be avoided to get large correlations between intracavity and reflected fields. We use a short, 0.33-mm long, cavity in order to keep a sufficient cavity bandwidth ($\Omega_{\rm cav}/2\pi = 700$ kHz) and to prevent laser frequency noise from limiting the displacement sensitivity. The cavity is operated in vacuum to increase the mechanical quality factors.

The cross-polarized signal and meter beams entering the cavity are provided by a Ti:sapphire laser working at 810 nm. As the cavity is birefringent (with a 5-MHz frequency mismatch between the two optical resonances), two acousto-optic modulators (AOM in Fig. 2) independently detune the two beams so that they both match the cavity resonance. The overall resonance is controlled by locking the laser frequency via a Pound-Drever-Hall technique: the incident signal beam is phase-modulated at 20 MHz by a resonant electro-optical modulator (REOM), and the resulting intensity modulation of the reflected beam provides the error signal. A mode cleaner cavity filters potential degradations of the spatial profile of both beams, while their intensities after the mode cleaner are stabilized by a servo-loop which drives the amplitude control of the AOMs.

The phase fluctuations $\delta\varphi_m^{\rm out}(t)$ of the reflected meter beam are monitored by a homodyne detection, with a local oscillator derived from the incident meter beam and phase-locked in order to detect the phase quadrature. For an incident power of 50 $\mu$W, one gets a shot-noise-limited displacement sensitivity of $2.7 \times 10^{-20}$ m/$\sqrt{\rm Hz}$ at frequencies above 200 kHz. Intensity fluctuations $\delta I_s^{\rm out}(t)$ of the reflected signal beam are monitored by a high-efficiency photodiode. We have carefully eliminated unwanted optical reflections so that the optical rejection of the double-beam system is higher than 35 dB: the phase

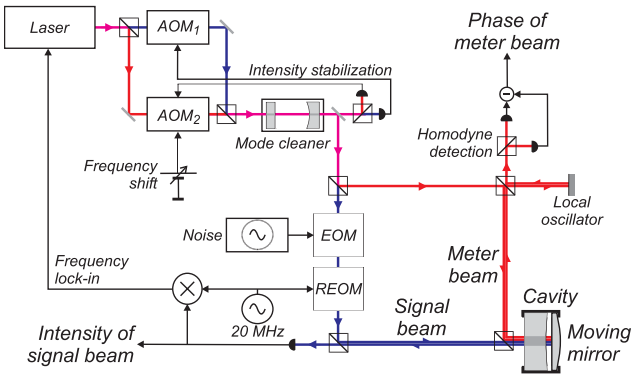


FIG. 2 (color online). Experimental setup. The laser beam is split in two orthogonally polarized beams, which are both sent into the moving mirror cavity. A resonant electro-optical modulator (REOM) is used to lock the laser onto the optical resonance via a Pound-Drever-Hall technique. The residual birefringence of the cavity is compensated by the frequency shift of two acousto-optic modulators (AOM), also used to stabilize the intensities of both beams after their spatial filtering by the mode cleaner cavity. A second EOM modulates the intensity of the signal beam to mimic quantum radiation-pressure noise. For simplicity, most polarizing elements are not shown.

fluctuations of the meter beam are insulated from the intensity fluctuations of the signal beam in such a way that observable effects of the signal beam are necessarily induced by intracavity radiation pressure.

In order to mimic the quantum fluctuations of radiation pressure, the signal beam is intensity-modulated with an electro-optic modulator (EOM) before entering the cavity to produce a classical intracavity radiation-pressure noise [22,24]. The digitized driving noise is centered at a frequency $\Omega_c$ close to the mechanical resonance frequency $\Omega_M$, and has a typical bandwidth of a few hundreds of Hz, larger than any bandwidth used in the correlations acquisition process. To generate a Gaussian intensity noise of the form $\delta I_s^{\rm in}(t) = A(t)\cos(\Omega_c t + \varphi(t))$, where $A(t)$ is a random function with a Gaussian distribution around 0 and $\varphi(t)$ a randomly distributed phase, we decompose the noise into its quadratures [25]:

$$\delta I_s^{\rm in}(t) = X_{I_s}^{\rm in}(t)\cos(\Omega_c t) + Y_{I_s}^{\rm in}(t)\sin(\Omega_c t). \qquad (2)$$

The quadratures are produced from a dual-channel arbitrary waveform generator Tektronix AFG3022B, and then summed to drive the EOM. The slowly-varying Gaussian noise functions $X_{I_s}^{\rm in}(t)$ and $Y_{I_s}^{\rm in}(t)$ are randomly generated by a computer and loaded into the generator as amplitude arrays.

The experiment is performed as follows. Both optical beams are locked onto the resonance of the cavity, with incident powers $P_s^{\rm in} = 150$ $\mu$W for the signal beam and $P_m^{\rm in} = 500$ $\mu$W for the meter. The EOM drives a classical radiation-pressure noise with an amplitude level as compared to thermal noise of $\sqrt{S_x^{\rm rad}/S_x^T} \simeq 5$, and with a center frequency $\Omega_c/2\pi = 1.123$ MHz, about 600 mechanical

linewidths below the mechanical resonance. The experimental signals are independently acquired by two spectrum analyzers Agilent MXA set in $I/Q$ mode in order to directly extract the quadratures $X_{I_s}^{\rm out}(t)$, $Y_{I_s}^{\rm out}(t)$, $X_{\varphi_m}^{\rm out}(t)$, and $Y_{\varphi_m}^{\rm out}(t)$ of the reflected signal intensity and meter phase, respectively. Both analyzers are locked at the same central frequency $\Omega_c$ with an analysis bandwith of 400 Hz, and synchronously triggered with the waveform generator. Temporal evolution of the quadratures are then acquired over a span time of 200 ms, equal to the scan time of the digitized amplitude-modulation arrays of the generator.

Figure 3 presents the observed phase-space trajectories: clear correlations are evident between the intensity noise of the signal beam (left) and the meter phase noise (right). Neglecting optical losses and irrelevant noises such as the quantum fluctuations of the meter beam, this can be interpreted from the following input-output relations for the fluctuations at frequency $\Omega_c$ [10]:

$$\delta I_s^{\rm out}[\Omega_c] = \frac{1+i\omega_c}{1-i\omega_c}\,\delta I_s^{\rm in}[\Omega_c], \tag{3}$$

$$\delta\varphi_m^{\rm out}[\Omega_c] = \frac{8\mathcal{F}}{\lambda(1-i\omega_c)}\,\delta x[\Omega_c], \tag{4}$$

where $\omega_c = \Omega_c/\Omega_{\rm cav}$, and $\delta x = \delta x_T + \delta x_{\rm rad}$ is the mirror motion, including the thermal noise and the radiation-pressure noise given by

$$\delta x_{\rm rad}[\Omega_c] = \frac{8\mathcal{F}}{\lambda(1-i\omega_c)}\hbar\chi[\Omega_c]\delta I_s^{\rm in}[\Omega_c], \tag{5}$$

where $\chi[\Omega_c]$ is the mechanical susceptibility of the moving mirror. The reflected signal intensity noise reproduces the incident one, with a global phase shift depending on $\omega_c$ [Eq. (3)], whereas the reflected meter phase reproduces the incident signal intensity $\delta I_s^{\rm in}$ via the mirror motion [Eqs. (4) and (5)]. It is superimposed to the thermal noise $\delta x_T$ of the mirror which is responsible for the small differences observed between the two phase-space trajectories in Fig. 3. Other noises such as the quantum phase noise of the incident meter beam, which limits the sensitivity of the displacement measurement, are negligible in our current setup with a level at least 15 dB below the thermal noise. Also note that the meter phase in Fig. 3 is calibrated in terms of the equivalent displacements of the moving mirror, with a typical amplitude of $10^{-15}$ m, and the curve has been rotated in phase space in order to compensate for the global phase shifts due to $\omega_c$ and to the mechanical response $\chi[\Omega_c]$.

We have obtained similar results with a center frequency $\Omega_c$ closer or equal to the mechanical resonance frequency. In that case, the resonance amplifies the radiation pressure and thermal displacements by a factor up to the quality factor $Q$, but the phase shift of the mechanical response across the resonance frequency has to be taken into account to deconvolve the observed data. We focus in the following on experimental results obtained at low frequency.

The results can be made more quantitative by computing the correlation coefficient $C_{I_s,\varphi_m}$ defined as

$$C_{I_s,\varphi_m} = \frac{|\langle \delta I_s^{\rm out}\delta\varphi_m^{\rm out\star}\rangle|^2}{\langle|\delta I_s^{\rm out}|^2\rangle\langle|\delta\varphi_m^{\rm out}|^2\rangle}, \tag{6}$$

where the brackets $\langle\ldots\rangle$ stand for a temporal average. We obtain a coefficient $C_{I_s,\varphi_m} \simeq 0.96$ for the data presented on Fig. 3, in perfect agreement with the value $(1 + S_x^T/S_x^{\rm rad})^{-1}$ deduced from Eqs. (3)–(5).

As in usual QND measurements [7], optomechanical correlations can also be quantified by the knowledge we gain on the signal intensity from the measurement of the meter phase. The resulting distribution is given by the conditional fluctuations

$$\delta I_{s|m} = \delta I_s^{\rm out} - \frac{\langle \delta I_s^{\rm out}\delta\varphi_m^{\rm out\star}\rangle}{\langle|\delta\varphi_m^{\rm out}|^2\rangle}\,\delta\varphi_m^{\rm out}. \tag{7}$$

Figure 4 presents the respective probability distributions in phase space for the uncorrected intensity fluctuations $\delta I_s^{\rm out}$ and the conditional ones $\delta I_{s|m}$, obtained as normalized histograms of the data of Fig. 3. The shrinking of the distribution is related to the lower conditional dispersion, reduced by a factor $\simeq 5$, as can be deduced from Eqs. (3)–(7):

$$\Delta I_{s|m} = \sqrt{1 - C_{I_s,\varphi_m}}\,\Delta I_s^{\rm out} \simeq 0.2\Delta I_s^{\rm out}. \tag{8}$$

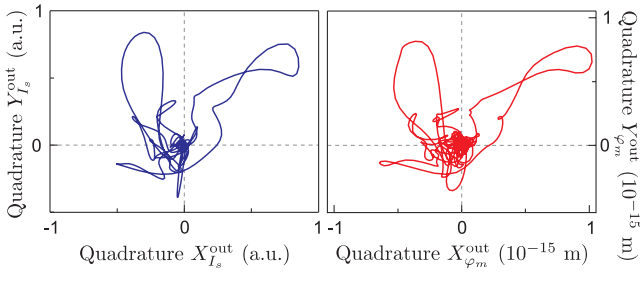


FIG. 3 (color online). Phase-space trajectories of the intensity noise of the signal beam (left) and the phase noise of the meter beam (right), in the case $\sqrt{S_x^{\rm rad}/S_x^T} \simeq 5$. The phase noise is calibrated as displacements of the moving mirror.

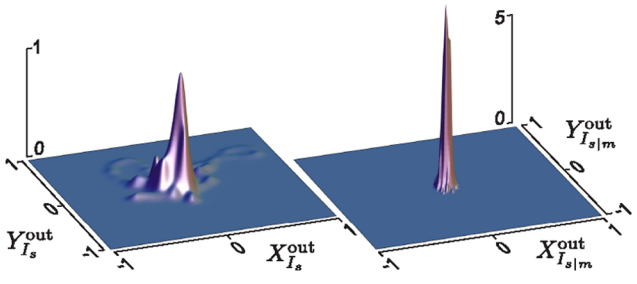


FIG. 4 (color online). Probability distributions in phase space of the signal intensity fluctuations $\delta I_s^{\rm out}$ (left) and of the conditional fluctuations $\delta I_{s|m}$ deduced from the meter measurement (right). Note the sharper peak, related to the lower conditional variance, and the factor 5 between the two vertical scales.

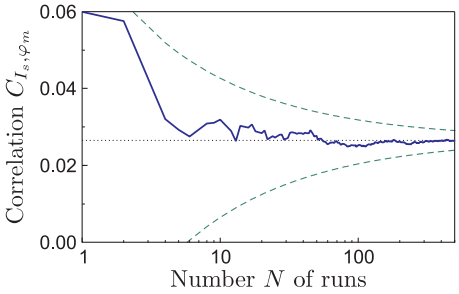


FIG. 5 (color online). Estimated optomechanical correlation coefficient $C_{I_s,\varphi_m}$ with respect to the number $N$ of independent 200-ms runs averaged. Dashed lines delineate the expected $1/\sqrt{N}$ statistical uncertainty region.

Our experimental setup enables to demonstrate optomechanical correlations even in the case of radiation-pressure effects smaller than thermal noise ($S_x^{\mathrm{rad}} \ll S_x^T$). In such a case, as the reflected meter phase fluctuations $\delta\varphi_m^{\mathrm{out}}$ are mainly related to random thermal noise, the correlation coefficient deduced from the temporal average of a single run has little meaning, and experimental values fluctuate from one run to the other. Nevertheless, repeating such runs and averaging all these experimental outcomes eventually yields a steady value.

Figure 5 presents the estimate of the correlation coefficient obtained with $S_x^{\mathrm{rad}}/S_x^T \simeq 0.03$, as a function of the number $N$ of runs averaged, up to $N = 500$. The resulting correlation coefficient tends to its small but nonzero expected value $(1 + S_x^T/S_x^{\mathrm{rad}})^{-1} \simeq 0.03$, with a statistical uncertainty at least 10-times smaller ($2.5 \times 10^{-3}$ for 500 averages).

Such correlations are still at the classical level but similar correlations are expected in the quantum regime at low temperature. Quantum radiation-pressure noise is about 30 dB below the classical noise used for Fig. 5, so that the ratio $S_x^{\mathrm{rad}}/S_x^T$ is equal to $0.03 \times 10^{-3} \times 300/4 \simeq 2 \times 10^{-3}$ for quantum noise at a cryogenic temperature of 4 K. The resulting quantum correlations could be recovered with 50 000 averages (uncertainty of $2.5 \times 10^{-4}$), with a total acquisition time of $50\,000 \times 200$ ms $\simeq 3$ h, easily reachable with our experimental setup.

We have thus demonstrated optomechanical correlations between two light beams. Averaging the experimental signal once working at low temperature should enable to retrieve the corresponding quantum correlations and hence demonstrate radiation-pressure noise. With an upgrade of our experimental setup, one can also envision radiation-pressure induced quantum optics experiments, such as optomechanical squeezing [8] or QND measurements [9,10].

We gratefully acknowledge the Laboratoire des Matériaux Avancés for the low-loss optical coatings and Matteo Barsuglia and Eric Chassande-Mottin for fruitful discussions. This work was partially funded by the Integrated Large Infrastructures for Astroparticle Science (ILIAS) of the Sixth Framework Program of the European Community.

[1] V. B. Braginsky and F. Ya. Khalili, *Quantum Measurement* (Cambridge University Press, Cambridge, England, 1992).
[2] C. Bradaschia *et al.*, Nucl. Instrum. Methods Phys. Res., Sect. A **289**, 518 (1990); A. Abramovici *et al.*, Science **256**, 325 (1992).
[3] C. M. Caves, Phys. Rev. D **23**, 1693 (1981); W. G. Unruh, in *Quantum Optics, Experimental Gravitation and Measurement Theory*, edited by P. Meystre and M. O. Scully (Plenum Press, New York, 1983), p. 647; P. Fritschel, Proc. SPIE Int. Soc. Opt. Eng. **4856**, 282 (2003).
[4] M. T. Jaekel and S. Reynaud, Europhys. Lett. **13**, 301 (1990); A. Luis and L. L. Sanchez-Soto, Phys. Rev. A **45**, 8228 (1992); A. Luis and L. L. Sanchez-Soto, Opt. Commun. **89**, 140 (1992).
[5] D. F. Walls, Nature (London) **306**, 141 (1983).
[6] R. E. Slusher, L. W. Hollberg, B. Yurke, J. C. Mertz, and J. F. Valley, Phys. Rev. Lett. **55**, 2409 (1985).
[7] P. Grangier, J. A. Levenson, and J.-P. Poizat, Nature (London) **396**, 537 (1998); N. Imoto, H. A. Haus, and Y. Yamamoto, Phys. Rev. A **32**, 2287 (1985); J.-F. Roch *et al.*, Phys. Rev. Lett. **78**, 634 (1997).
[8] C. Fabre *et al.*, Phys. Rev. A **49**, 1337 (1994).
[9] K. Jacobs, P. Tombesi, M. J. Collett, and D. F. Walls, Phys. Rev. A **49**, 1961 (1994).
[10] A. Heidmann, Y. Hadjar, and M. Pinard, Appl. Phys. B **64**, 173 (1997).
[11] Y. Hadjar, P.-F. Cohadon, C. G. Aminoff, M. Pinard, and A. Heidmann, Europhys. Lett. **47**, 545 (1999).
[12] P.-F. Cohadon, A. Heidmann, and M. Pinard, Phys. Rev. Lett. **83**, 3174 (1999).
[13] I. Tittonen *et al.*, Phys. Rev. A **59**, 1038 (1999).
[14] O. Arcizet *et al.*, Phys. Rev. Lett. **97**, 133601 (2006).
[15] O. Arcizet, P.-F. Cohadon, T. Briant, M. Pinard, and A. Heidmann, Nature (London) **444**, 71 (2006).
[16] S. Gigan *et al.*, Nature (London) **444**, 67 (2006).
[17] T. Corbitt *et al.*, Phys. Rev. Lett. **99**, 160801 (2007).
[18] J. D. Thompson *et al.*, Nature (London) **452**, 72 (2008).
[19] A. Schliesser, O. Rivière, G. Anetsberger, O. Arcizet, and T. J. Kippenberg, Nature Phys. **4**, 415 (2008).
[20] R. G. Knobel and A. N. Cleland, Nature (London) **424**, 291 (2003); M. D. LaHaye, O. Buu, B. Camarota, and K. C. Schwab, Science **304**, 74 (2004).
[21] D. Rugar, R. Budakian, H. J. Mamin, and B. W. Chui, Nature (London) **430**, 329 (2004).
[22] T. Caniard, P. Verlot, T. Briant, P.-F. Cohadon, and A. Heidmann, Phys. Rev. Lett. **99**, 110801 (2007).
[23] T. Briant, P.-F. Cohadon, A. Heidmann, and M. Pinard, Phys. Rev. A **68**, 033823 (2003).
[24] C. M. Mow-Lowry *et al.*, Phys. Rev. Lett. **92**, 161102 (2004).
[25] T. Briant, P.-F. Cohadon, M. Pinard, and A. Heidmann, Eur. Phys. J. D **22**, 131 (2003).